AMERICAN SOCIETY FOR MICROBIOLOGY | Journal of Bacteriology

Succinic Semialdehyde Promotes Prosurvival Capability of *Agrobacterium tumefaciens*

Chao Wang,[a,b] Desong Tang,[c] Yong-Gui Gao,[a,c] Lian-Hui Zhang[a,d]

Institute of Molecular and Cell Biology, Singapore, Singapore[a]; National Cancer Centre Singapore, Singapore, Singapore[b]; School of Biological Sciences, Nanyang Technological University, Singapore, Singapore[c]; Guangdong Province Key Laboratory of Microbial Signals and Disease Control, South China Agricultural University, Guangzhou, China[d]

ABSTRACT

Succinic semialdehyde (SSA), an important metabolite of γ-aminobutyric acid (GABA), is a ligand of the repressor AttJ regulating the expression of the *attJ-attKLM* gene cluster in the plant pathogen *Agrobacterium tumefaciens*. While the response of *A. tumefaciens* to GABA and the function of *attKLM* have been extensively studied, genetic and physiological responses of *A. tumefaciens* to SSA remain unknown. In combination with microarray and genetic approaches, this study sets out to explore new roles of the SSA-AttJKLM regulatory mechanism during bacterial infection. The results showed that SSA plays a key role in regulation of several bacterial activities, including C_4-dicarboxylate utilization, nitrate assimilation, and resistance to oxidative stress. Interestingly, while the SSA relies heavily on the functional AttKLM in mediating nitrate assimilation and oxidative stress resistance, the compound could regulate utilization of C_4-dicarboxylates independent of AttJKLM. We further provide evidence that SSA controls C_4-dicarboxylate utilization through induction of an SSA importer and that disruption of *attKLM* attenuates the tumorigenicity of *A. tumefaciens*. Taken together, these findings indicate that SSA could be a potent plant signal which, together with AttKLM, plays a vital role in promoting the bacterial prosurvival abilities during infection.

IMPORTANCE

***Agrobacterium tumefaciens* is a plant pathogen causing crown gall diseases and has been well known as a powerful tool for plant genetic engineering. During the long history of microbe-host interaction, *A. tumefaciens* has evolved the capabilities of recognition and response to plant-derived chemical metabolites. Succinic semialdehyde (SSA) is one such metabolite. Previous results have demonstrated that SSA functions to activate a quorum-quenching mechanism and thus to decrease the level of quorum-sensing signals, thereby avoiding the elicitation of a plant defense. Here, we studied the effect of SSA on gene expression at a genome-wide level and reported that SSA also promotes bacterial survival during infection. These findings provide a new insight on the biological significance of chemical signaling between agrobacteria and plant hosts.**

During the long history of bacteria-plant interactions, *Agrobacterium tumefaciens* has evolved sophisticated signal cross talk mechanisms to ensure successful infection. Previous studies have shown that the bacterium can perceive a wide variety of plant-derived metabolites and transduce them to regulate a particular set of bacterial genes (1). Succinic semialdehyde (SSA), the metabolite of γ-aminobutyric acid (GABA), is one such metabolite. SSA has been implicated in the regulation of bacterial quorum-quenching activity, the starvation response, and GABA catabolism and consequently affects the severity of plant symptom development (2–5).

SSA exerts its function through the proteins encoded by the *attJ-attKLM* (also named *bclR-bclABC*) genes. In *A. tumefaciens*, *attJ* and *attKLM* are localized at the same locus in opposite orientations, where *attKLM* constitute a cotranscribed operon. In the *attKLM* operon, *attK* encodes a semialdehyde dehydrogenase, *attL* encodes an alcohol dehydrogenase, and *attM* encodes a lactonase. These enzymes convert gamma-butyrolactone (GBL) sequentially to gamma-hydroxybutyrate (GHB), SSA, and succinic acid (SA), the last of which is integrated into the tricarboxylic acid (TCA) cycle (3, 6, 7). These enzymes also enable *A. tumefaciens* to metabolize γ-butyrolactone (GABA) as a sole carbon source for bacterial growth. In addition, AttM efficiently degrades the quorum-sensing (QS) signal acylated homoserine lactone (AHL) and controls the replication and conjugation of Ti plasmid (8, 9). The transcription of *attKLM* is repressed by AttJ. AttJ, an IclR-type transcription factor, physically binds to the promoter region of *attKLM* and tightly represses its expression. The repression of AttJ is relieved in the presence of SSA (3). It has been demonstrated that SSA, serving as the cognate ligand, directly binds to AttJ and attenuates its association with the promoter of *attKLM*. Crystal structural analysis of AttJ further indicates that SSA regulates its DNA-binding activity through protein oligomerization (10). Thus, supplementation of SSA induces the expression of *attKLM*, while depletion of SSA suppresses *attKLM* transcription (2–4).

In addition to the role of SSA in activation of *attKLM* transcriptional expression, several lines of evidence suggest that SSA may also play other regulatory roles. First, the IclR-type transcrip-

Received 15 May 2015 **Accepted** 10 December 2015

Accepted manuscript posted online 11 January 2016

Citation Wang C, Tang D, Gao Y-G, Zhang L-H. 2016. Succinic semialdehyde promotes prosurvival capability of *Agrobacterium tumefaciens*. J Bacteriol 198:930–940. doi:10.1128/JB.00373-15.

Editor: V. J. DiRita

Address correspondence to Lian-Hui Zhang, lianhui@imcb.a-star.edu.sg.

Supplemental material for this article may be found at http://dx.doi.org/10.1128/JB.00373-15.

tional regulators are known to regulate a variety of bacterial activities ranging from carbon metabolism to virulence expression (11). For example, the regulator IclR represses the genes encoding acetate utilization in *Escherichia coli*, KdgR is involved in exoenzyme production in *Erwinia chrysanthemi*, and SggR is associated with sporulation development in *Streptomyces coelicolor* (12–16). Regulation of quorum quenching by AttJ in *A. tumefaciens* adds another new role of the IclR-type regulators in bacteria. In this regard, it is interesting that an *in silico* search found more than 16 IclR-type regulators in the genome of *A. tumefaciens*, suggesting that IclR-type regulators may regulate a wide range of biological activities in this bacterial species. It is not clear yet whether SSA may also influence the functionality of these AttJ homologues. Second, SSA is produced by both eukaryotes and prokaryotes and is implicated in various biological functions. In human, abnormal accumulation of SSA exerts a wide range of adverse effects within the nervous system (17, 18). In *Arabidopsis*, a defect in SSA degradation enhances cell death under stressful conditions (19, 20). In *Saccharomyces cerevisiae*, mutation of SSA dehydrogenase increases the susceptibility of the microbe to salinity and osmotic and oxidative stresses (21). In *Ralstonia eutropha*, disruption of SSA metabolism impairs the ability of the bacterium to metabolize 4-hydroxybutyric acid as the sole carbon source (22). Third, although current knowledge indicates that *A. tumefaciens* takes up the plant signaling molecule GABA through a specific importer and converts it to produce SSA (23), a recent study showed that the expression of *attKLM* could be induced in the presence of wounded plant tissues even if the *A. tumefaciens* importer of GABA is disrupted (4), suggesting that SSA could be a specific plant signal that can be recognized by the bacterial cells and is worthy of further investigations.

In this study, we conducted microarray analysis to test the impact of SSA on transcriptional expression of the genes in *A. tumefaciens*. Based on the microarray results, we further performed a series of genetic and biochemical analyses to explore the roles of SSA and regulatory mechanisms in modulation of bacterial physiology. Our results identified a few new functions regulated by SSA, including utilization of C_4-dicarboxylates, nitrate assimilation, and reactive oxygen species (ROS) resistance. In addition, we showed that functional AttKLM are required for SSA-mediated nitrate assimilation, ROS resistance, and virulence, which strongly suggests that *A. tumefaciens* could recognize and utilize SSA as a potent plant signal to modulate its survival capability during pathogen-host interactions.

MATERIALS AND METHODS

Bacterial strains and culture conditions. The bacterial strains used in this study are listed in Table S1 in the supplemental material. *E. coli* strains were grown at 37°C in LB medium. *A. tumefaciens* strains were grown at 28°C in LB or in BM medium (8). For the carbon and nitrogen utilization experiments, bacterial strains specified in the legend to Fig. 2B were freshly grown on LB agar plates. After 16 h, bacterial cells were directly scraped from the plates and suspended in BM medium without carbon or nitrogen sources (10 mM K_2HPO_4, 10 mM KH_2PO_4, 2.5 mM NaCl, 2 mM $MgSO_4 \cdot 7H_2O$, 0.7 mM $CaCl_2$, 9 μM $FeSO_4 \cdot 7H_2O$, pH 7.2). D-Mannitol (0.2%) was the carbon source when KNO_3 (0.2%) was used as the sole nitrogen source, and $(NH_4)_2SO_4$ was the nitrogen source when malate (0.2%) was the sole carbon source. Chemicals used in this study were purchased from Sigma, and the final concentrations were 0.2 mM unless otherwise specified. The bacterial cells (10 ml of liquid culture) were grown in 50-ml Falcon tubes, and the initial inoculation was at an optical density at 600 nm (OD_{600}) of 0.05, with shaking at 220 rpm at 28°C. The OD_{600} values were measured after 24 h of growth. The results are presented as means ± standard deviations (SD) based on three experimental repeats.

RNA preparation for RT-PCR and microarray hybridization. *A. tumefaciens* strain C58 was used for microarray analysis in this study because of the availability of its genome sequence (24, 25). Bacterial cells were cultivated in BM medium at 28°C with shaking at 200 rpm and collected for RNA isolation when the OD_{600} reached ~0.4. The total RNAs were isolated with an RNeasy minikit (Qiagen), and the residual DNAs were removed by RNase-free DNase I (Promega). The absence of residual DNAs was confirmed by the lack of PCR products after 35 cycles of PCR amplification with primers specific for the 16S RNA gene. RNA integrity was monitored by agarose gel electrophoresis, and RNA concentration was measured by a Nanodrop ND-1000 instrument (Nanodrop Technologies). For reverse transcription-PCR (RT-PCR), an aliquot of 0.2 μg of total RNA was serially diluted 10-fold and used as the template for one-step RT-PCR analysis (Qiagen). PCR primers used for RT-PCR analysis are listed in Table S1 in the supplemental material.

For microarray hybridization, cDNA was synthesized by using SuperScript II reverse transcriptase (Invitrogen) with 10 μg of total RNA and purified by phenol extraction following RNase digestion (NimbleGen Systems). The cDNA molecules were then fragmented into 50 to 200 nucleotides by partial digestion using DNase I (Promega) and labeled with biotin for microarray hybridization. The DNA microarray chips were synthesized by NimbleGen Systems (Madison, WI), and each chip included 4,661 open reading frames (ORFs) of the compiled genome sequence of *A. tumefaciens* strain C58 (University of Washington). Each ORF was represented by 20 unique and perfectly matched oligonucleotides (24-mer), which were *in situ* synthesized on the glass slide in duplicate. Therefore, each chip included two sets of 93,220 synthesized oligonucleotides, representing the 4,661 annotated ORFs. Labeled cDNA samples were individually hybridized to the *A. tumefaciens* C58-specific chips according to the NimbleGen standard procedures.

Microarray data analysis. Following hybridization, the arrays were scanned, and the median signal intensity for each probe on the array was calculated by using NimbleGen's extraction software. For each probe pair, the difference between the perfect match (PM) and mismatch (MM) signal intensities was calculated together with the Tukey biweight mean from the 20 probe pairs for each ORF. The data were then further processed with the tools provided by Bioconductor (http://www.bioconductor.org). Gene calls were generated using the robust multiarray average (RMA) algorithm (26). The RMA value is the log to base 2, and ratios of SSA-treated to untreated cDNAs were calculated based on normalized data so that the ratio of signal from the SSA-induced sample to that of the untreated sample for a given ORF should represent the relative abundance of the transcripts of that ORF under the two conditions. Unless otherwise stated, the annotated ORFs were retrieved from the BioCyc Database Collection (http://biocyc.org/server.html).

Gene cloning and gene deletion. DNA manipulation and transformation of *E. coli* were performed according to standard procedures. To generate the suicide plasmid construct pK18-Δ*dctA*, two DNA fragments were amplified from *A. tumefaciens* C58 with the primer pair 5′-GCTCTAGATGACAGAGGACTGCGTG-3′ and 5′-CGGGATCCCGGTGATGGTCTGCTCATG-3′ and the pair 5′-CGGGATCCTTCTGCTGCTCGTGG-3′ and 5′-GCTCTAGAAACAGACCGCGAAGACG-3′. After enzymatic digestion and ligation of T4 DNA ligase, the reaction mixture was aliquoted for another round of PCR amplification using the primer pair 5′-GCTCTAGATGACAGAGGACTGCGTG-3′ and 5′-GCTCTAGAAACAGACCGCGAAGACG-3′. DNA fragments with predicted sizes were then recovered from a 1% agarose gel, treated with XbaI, and linked into the vector pK18mobsacB that was also treated with XbaI. The resulting pK18-Δ*dctA* plasmid was screened by PCR and confirmed by DNA sequencing. Similarly, the pK18-Δ*dctB1* plasmid was constructed by using the following PCR primers: the pair

5′-GCTCTAGAAATACGCATGCCAGACTTGC-3′ and5′-GCTCTAGAGCATAATGTTCGGACATGC-3′ and the pair 5′-GCTCTAGACTCGGTCTTGGCCTCGTC-3′ and 5′-GCTCTAGAACATCCACATCCGTATCGG-3′.

In-frame deletion of *dctA* and *dctB1* in *A. tumefaciens* A6 was carried out according to a modification of a procedure described previously (27). Briefly, the transconjugants were screened on the BM medium containing kanamycin. The purified transconjugants were further selected on fresh BM agar plates containing 5% sucrose. The potential deletion mutants were then identified by loss of kanamycin resistance and PCR confirmation.

NADH/NAD and NADPH/NADP ratio measurement. NADH/NAD and NADPH/NADP ratios were, respectively, measured by NAD/NADH and NADP/NADPH quantification kits (Sigma-Aldrich). Briefly, fresh bacteria were cultivated in minimal medium with or without SSA treatment. Ratios of free NADH/NAD and NADPH/NADP were determined with the method recommended by the manufacturer. The fold changes in the NADH/NAD and NADPH/NADP ratios were derived by dividing the NADH/NAD or NADPH/NADP ratio with SSA induction by the respective ratio without SSA induction.

H_2O_2 resistance assay. *A. tumefaciens* strains C58 and A6 were grown in LB medium with or without SSA to an OD_{600} of ~0.5 and used for subsequent experiments. For an H_2O_2 sensitivity assay, the cell cultures were added with H_2O_2 at a final concentration of 20 mM and grown at 28°C with shaking at 200 rpm for 25 min. A serial dilution of bacterial cells was immediately prepared and plated on LB agar plates. Colonies were enumerated after growth for 3 days, and the survival rate of each strain treated with H_2O_2 was calculated relative to that of the blank control.

Tumorigenicity assay. Fresh bacterial cells grown in LB were collected and washed once and resuspended in phosphate-buffered saline (PBS) buffer at an OD_{600} of 1.0. The bacterial suspension was diluted as indicated (see Fig. 7A), and 5 μl of bacterial samples was used to infect leaves of *Kalanchoe daigremontiana*. The growth conditions and calculation of tumor size were described previously (4, 28).

RESULTS

Experimental design and microarray measurement. For identification of the genes modulated by SSA on a genome-wide scale, a DNA microarray was performed on *A. tumefaciens* C58 in the presence or absence of SSA. Given that the bacterial intracellular SSA could transiently accumulate upon entry into stationary phase (3), we treated the cell culture with SSA at the early stage (OD_{600} of 0.5), and RNA samples were prepared from exponentially growing cells to minimize the interference of endogenous SSA. Thus, the results obtained from this study may miss those genes whose regulation requires a specific factor(s) present only in the late growth phase.

The microarray analysis showed that the transcriptional levels of 325 genes, falling into 14 functional categories (Fig. 1), were increased by more than 2-fold upon SSA treatment (see Table S2 in the supplemental material). Among these genes, 20% are the ORFs encoding hypothetical proteins. The remaining are the genes associated with protein synthesis, transportation, and energy metabolism, representing 17%, 12%, and 13%, respectively, of the total. In contrast, only 20 genes showed a >1.5-fold decrease (Fig. 1; see also Table S3 in the supplemental material). These results suggest that SSA may primarily activate rather than suppress gene expression under our experimental conditions.

The microarray data showed that the genes most strongly induced by SSA were *attM*, *attL*, and *attK*, with induction ratios of 21-, 14-, and 9-fold, respectively (see Table S2 in the supplemental material), which is highly consistent with the previous results that SSA is the inducer of the *attMLK* operon (3). In addition to *attKLM*, the transcriptional expression of *attJ* was also increased by about 3.7-fold (see Table S2), suggesting an SSA-dependent autoregulatory mechanism that governs AttJ transcription.

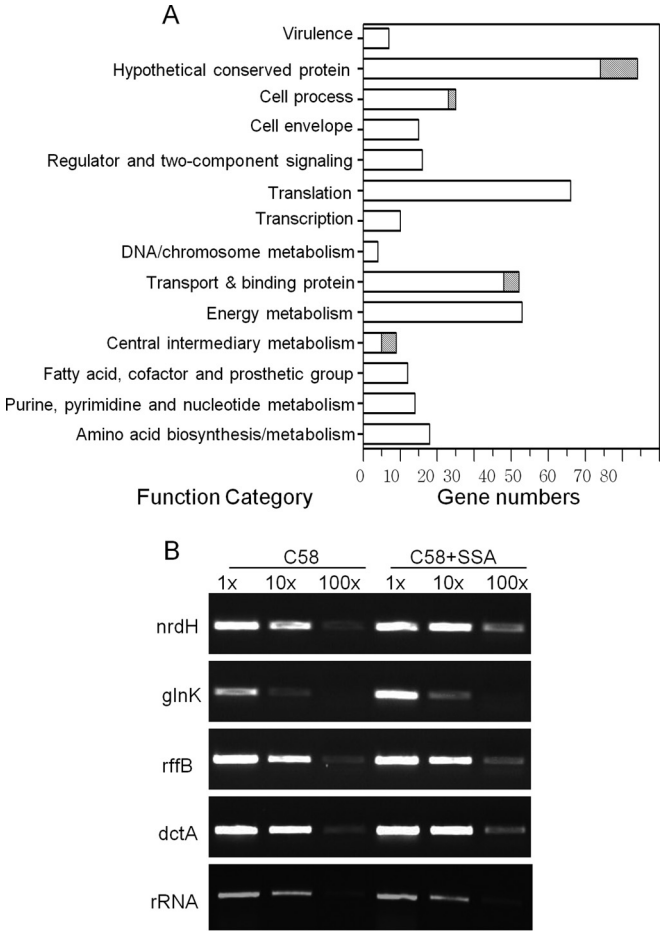

FIG 1 Microarray analyses of *A. tumefaciens* A6 with or without SSA treatment. (A) Functional groups and the numbers of genes whose expression levels were upregulated (open bars) or repressed (shaded bars) by external addition of SSA. Genes are categorized into functional classes based on the annotation available from the *A. tumefaciens* genome sequences (24, 25). (B) Validation of microarray results by RT-PCR.

SSA promotes C_4-dicarboxylate utilization. The metabolism of C_4-dicarboxylates, such as succinate and malate, has received considerable attention in rhizobia because of its important role in promoting bacterial survival in plant hosts (29). Rhizobial species take up these compounds via a high-affinity C_4-dicarboxylate transporter encoded by the *dctA* gene (30). In *Sinorhizobium meliloti*, transcription of *dctA* is induced by C_4-dicarboxylates via the DctB/DctD two-component system (31). Additionally, the sigma factor σ^{54} is also implicated in the regulation of *dctA* (32). Analysis of the *A. tumefaciens* genome sequences revealed not only *dctA* but also two copies of the σ^{54} gene *rpoN* and two sets of the *dctB-dctD* paralogs (Fig. 2A). Our microarray data showed that *dctA* transcription was induced up to about 5.8 times by SSA treatment, which was further verified by semiquantitative RT-quantitative PCR (RT-qPCR) analyses (Fig. 1B). In contrast, the mRNA levels of *dctB-dctD* and the nitrogen-limiting sigma factor σ^{54} remained

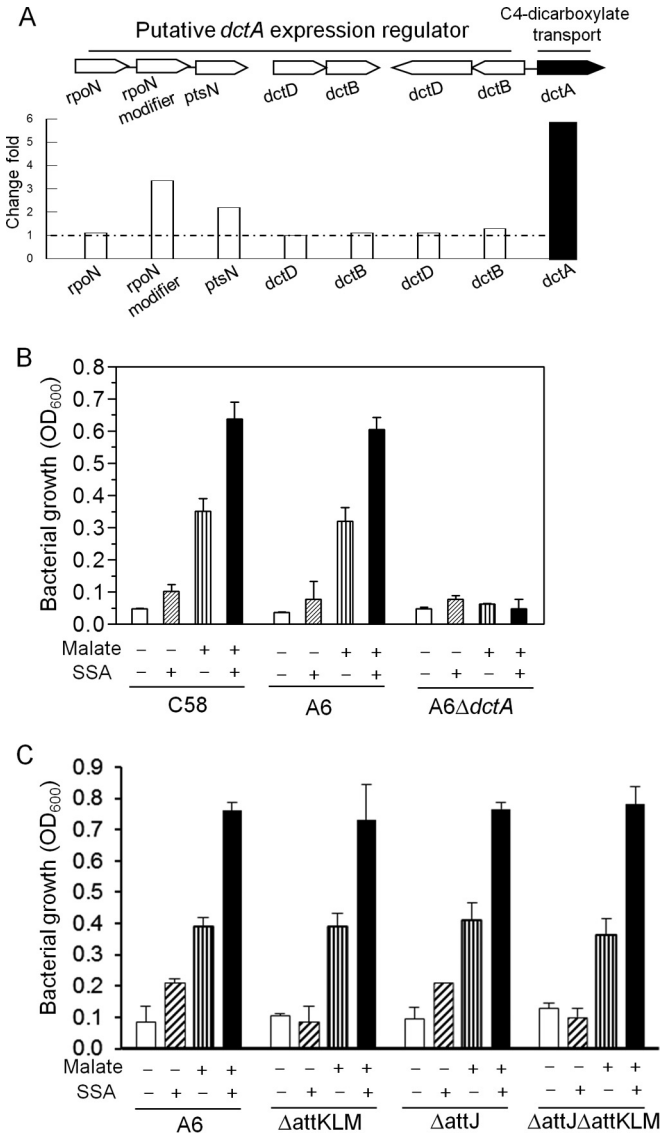

FIG 2 SSA promotes C_4-dicarboxylate utilization in *A. tumefaciens*. (A) Organization of C_4-dicarboxylate transporter gene clusters and their induction profiles in the microarray. The gene clusters are composed of a *dctA* transporter gene, three *rpoN*-related regulators, and two sets of *dctB-dctD* genes encoding two-component regulatory systems. The arrows indicate the direction of transcription. Fold change was calculated based on the average readings of two repeated microarrays. (B) Growth of *A. tumefaciens* C58, A6, and the A6 *dctA* deletion mutant (Δ*dctA* strain) using malate as the sole carbon source with or without SSA. (C) Growth of *A. tumefaciens* A6 and its mutant using malate as the sole carbon source with or without SSA. −, no chemical addition; +, chemical addition. Error bars denote standard deviations.

unchanged (Fig. 2A; see also Table S2 in the supplemental material).

Given that DctA is essential for the growth of *A. tumefaciens* C58 with C_4-dicarboxylates as the sole carbon source (30), induction of *dctA* by SSA suggests that SSA may promote C_4-dicarboxylate utilization in this bacterial species. Therefore, we monitored the bacterial growth with malate as the sole carbon source. Results shown in Fig. 2B indicate that the *A. tumefaciens* strains C58 and A6 grew poorly when malate was used as the sole carbon source, with the OD_{600} reaching about 0.3 after 24 h of growth. In the presence of SSA, however, the growth of the two bacterial strains was substantially boosted, with the OD_{600} reaching approximately 0.65. Given that SSA alone could hardly support bacterial growth, these results indicate that SSA is able to promote C_4-dicarboxylate utilization in *A. tumefaciens*. When the *dctA* gene is deleted in the octopine-type A6 strain, the bacterial cells failed to grow with either SSA or malate as the only carbon source (Fig. 2B). When mannitol or fumarate was used as a carbon source, however, no significant change was recorded in the growth rates between the *dctA* deletion mutant and the wild-type strain, and both grew well. Taken together, these results indicate that SSA might promote malate utilization by increasing the expression level of its transporter DctA although it could not be ruled out at this stage that SSA may also function through other unknown pathways.

To examine whether *attJ-attKLM* are involved in the SSA-mediated C_4-dicarboxylate utilization, we used the corresponding mutants to conduct growth tests. As shown in Fig. 2C, the wild-type and Δ*attJ* strains grew poorly when SSA was added under these experimental conditions, whereas no growth was recorded for the Δ*attKLM* and Δ*attJ*Δ*attKLM* strains. These results suggest that *attKLM* are essential for SSA-supported bacterial growth. When malate was added alone as the sole carbon source, however, all the tested mutants exhibited growth rates similar to the growth rate of the wild type, indicating that neither *attJ* nor *attKLM* is involved in malate metabolism. Furthermore, when SSA and malate were added together, all the tested mutants grew well, with growth at a rate comparable to that of the wild type. Taken together, these results suggest that SSA-promoted malate utilization is dependent on the DctA transporter but independent of the functions encoded by the *attJ-attKLM* gene cluster.

SSA promotes nitrate assimilation. In bacteria, the nitrate assimilation pathway generally involves four steps (33). Nitrate is first reduced by a nitrate reductase into nitrite and then ammonia, which is further converted into glutamate by glutamine synthase and glutamate synthase (Fig. 3A). Microarray results showed that the genes encoding nitrate reductase, ammonia transportation, and glutamine synthase were significantly induced by SSA treatment (Fig. 3B), suggesting that SSA may be involved in nitrate assimilation. With validation by RT-PCR (Fig. 1B), we examined the growth of *A. tumefaciens* by using potassium nitrate (KNO_3) as the sole nitrogen source and mannitol as the carbon source. As shown in Fig. 3C, both the nopaline strain C58 and the octopine strain A6, similar to other rhizobial species, could use KNO_3 as the sole nitrogen source for growth (34). Addition of SSA to the same medium significantly promoted the growth of both strain C58 and strain A6. As a control, SSA alone, as expected, could not support bacterial growth in the absence of a nitrogen source. Moreover, when the nitrogen source was changed to $(NH_4)_2SO_4$, SSA failed to promote bacterial growth (see Fig. S1 in the supplemental material). Cumulatively, the above findings established the specific role of SSA in promoting nitrate assimilation in *A. tumefaciens* through transcriptional upregulation of the related genes.

AttK and AttL, but not AttM, are responsible for the SSA-mediated nitrate assimilation. To examine whether AttJ-AttKLM are involved in the SSA-mediated nitrate assimilation, we used the *attJ-attKLM* mutants to investigate bacterial growth using nitrate as the sole nitrogen source. Results showed that the wild-type strain and its mutants grew at similar rates without SSA. In contrast, addition of SSA significantly boosted the growth of the wild-type strain and the Δ*attJ* mutant, whereas the Δ*attKLM* and

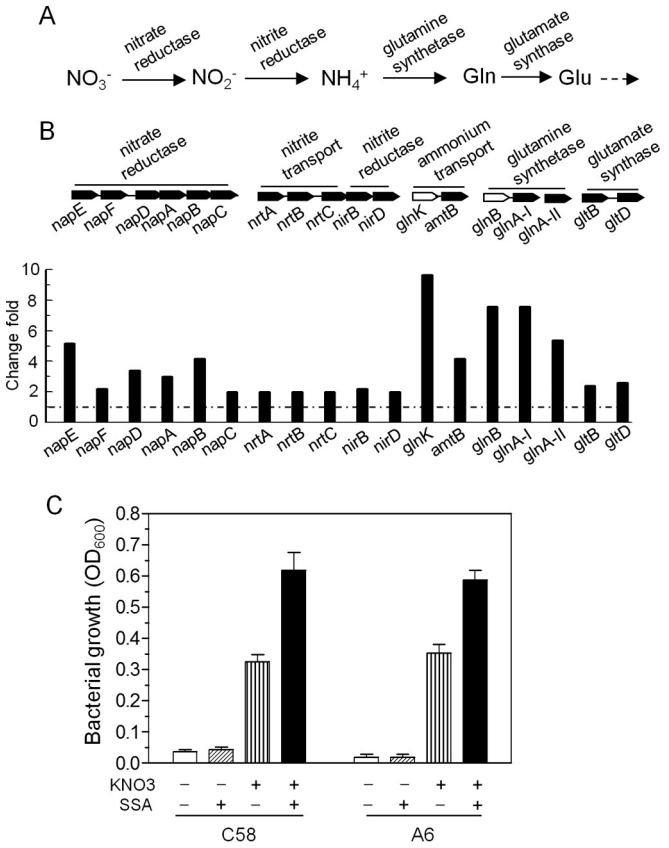

FIG 3 SSA promotes nitrate assimilation in *A. tumefaciens*. (A) The metabolic pathway for nitrate assimilation in *A. tumefaciens*. Glu, glutamate; Gln, glutamine. (B) Arrangement of nitrate assimilatory gene clusters and their induction profiles in microarray. The clusters are composed of the genes encoding putative nitrate reductase, nitrite reductase, glutamine synthetase, glutamate synthase, and related transporters and regulators (open columns). The arrows indicate the transcriptional direction. (C) Growth of *A. tumefaciens* using KNO_3 as the sole nitrogen source with or without SSA treatment. The fresh bacteria from LB agar were resuspended in PBS and then inoculated at a ratio of 1% in a defined medium. −, no chemical addition; +, chemical addition. Error bars denote standard deviations.

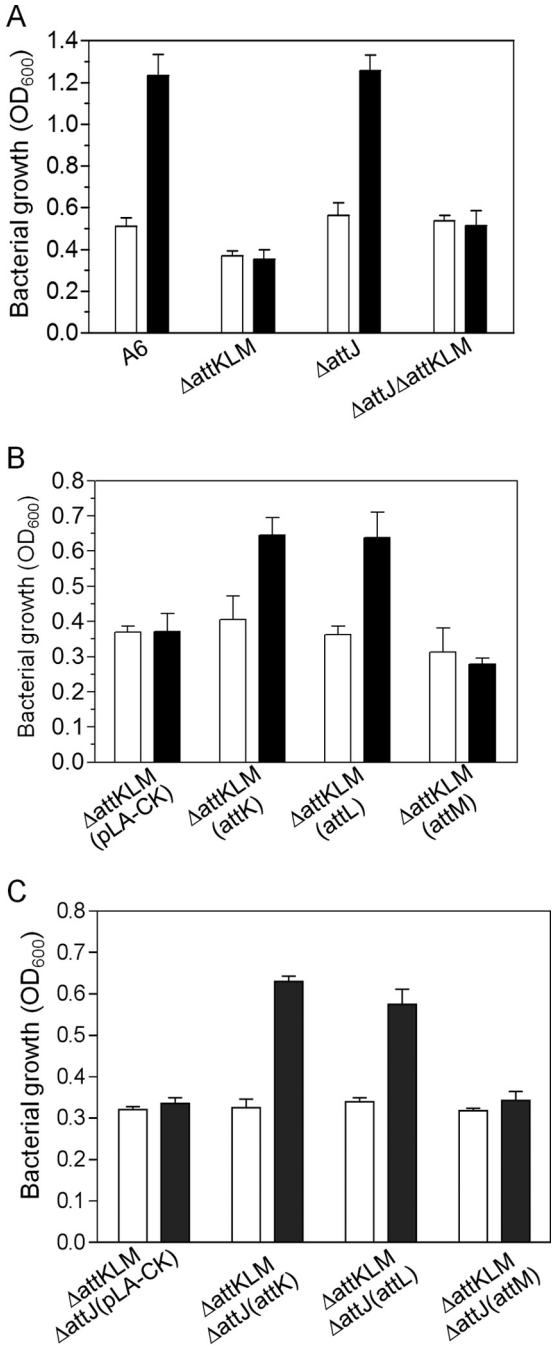

FIG 4 AttKL, but not AttJ and AttM, was required for nitrate utilization in *A. tumefaciens*. Bacterial growth of *A. tumefaciens* A6 and its mutants was determined using KNO_3 as the sole nitrogen source. OD_{600} values were recorded for cells cultured with shaking at 220 rpm at 28°C for 24 h. Open bars, no SSA added; filled bars, SSA added. Error bars denote standard deviations.

Δ*attKLM* Δ*attJ* mutants failed to respond to SSA and had growth rates similar to those in the absence of SSA (Fig. 4A). To determine which gene in *attKLM* is responsible for the SSA-promoted nitrate assimilation, we constitutively expressed the corresponding individual genes in the Δ*attKLM* mutant. Results showed that expression of *attK* or *attL* could partially restore the bacterial response to the level of that with SSA treatment (Fig. 4B). In contrast, overexpression of *attM* displayed no significant effect as the Δ*attKLM* (*attM*) strain grew similarly with or without SSA (Fig. 4B). We also expressed *attK*, *attL*, and *attM* separately in the Δ*attKLM* Δ*attJ* strain in which *attJ* was further mutated in the background of Δ*attKLM*. Similar to the results for the Δ*attKLM* strain, overexpression of *attK* or *attL* but not of *attM* restored the bacterial response to SSA (Fig. 4C). Sequence analyses indicate that both *attK* and *attL* encode homologues of dehydrogenases, but it is not yet clear how these two dehydrogenases are involved in nitrate utilization.

In addition to AttK, AldH was also demonstrated to convert SSA to SA, and inactivation of *aldH* in the Δ*attK* strain led to accumulation of SSA in *A. tumefaciens* (3, 7). To test the potential involvement of AldH in assimilation of C_4-dicarboxylates and nitrates, the *aldH* gene was deleted from the mutant Δ*attKLM* strain, and bacterial growth was examined accordingly. With nitrate as the sole nitrogen source, the growth of the mutant lacking both *attK* and *aldH* was indistinguishable from that of the mutant lacking only *attK* (see Fig. S2 in the supplemental material). However, no growth of the Δ*attKLM* Δ*aldH* strain was observed with exog-

enous addition of SSA, even at a concentration as low as 20 μM (see Fig. S2). These results suggest the *attK aldH* double deletion mutant was highly sensitive to the toxicity of SSA. Further experiments are required to study the biological significance of AldH in *A. tumefaciens* physiology.

SA promotes nitrate utilization in an *attJ-attKLM*-independent manner. It has been proposed that *attK* functions as a dehydrogenase which converts SSA into SA for the tricarboxylic acid (TCA) cycle. The requirement of *attKLM* for SSA-promoted nitrate assimilation tempted us to test whether SA, the hydrolyzing product of SSA, could also induce bacteria to use nitrate as the sole nitrogen source. The results showed that, similar to SSA, SA promoted the bacterial growth of the wild-type strain and the *attJ* mutant to an extent that was statistically significant, but growth was less than that with SSA ($P < 0.005$, *t* test). However, SA also promoted bacterial growth of Δ*attKLM* and Δ*attKLM* Δ*attJ* strains, which was different from the results with SSA (Fig. 5A). As a comparison, we further investigated whether other carbon sources could also promote bacterial growth with nitrate as the sole nitrogen source. The results showed that only SSA and its product SA could promote nitrate assimilation by the wild-type strain A6, whereas other C_4-dicarboxylates, including malate and α-ketoglutaric acid, and common carbon sources, such as mannitol, glucose, and fructose, failed to promote nitrate assimilation (Fig. 5B). Altogether, these results suggest that SA, like its precursor SSA, is able to induce bacteria to assimilate nitrate for growth, and this promotion effect of SA is independent of the *attJ-attKLM* operon.

In *A. tumefaciens*, AttK is an enzyme supposed to convert SSA into SA, and this conversion is accompanied by the oxidation of NAD(P)H. Results showing that SA promoted bacterial growth encouraged us to examine the changes in abundance of NAD(P)H in bacterial cells in the presence or absence of SSA. First, we treated bacterial cells with SSA and determined the changes in the NADH/NAD and NADPH/NADP ratios. As shown in Fig. 5C, no significant change was recorded for the NADH/NAD ratio in wild-type strain A6 and its *attJ-attKLM* mutant with and without SSA treatment. For the NADPH/NADP ratio, however, addition of SSA led to a 3-fold increase in the wild-type strain over the level of the blank control without SSA. In the Δ*attJ* mutant, the SSA-induced increase in the NADPH/NADP ratio appeared even higher than that of the wild type, with about a 4.5-fold increase above the level of the control without SSA. When *attKLM* was mutated, however, this SSA-stimulated increase vanished, as shown by results for the Δ*attKLM* and Δ*attKLM* Δ*attJ* mutant strains (Fig. 5C). Although purified AttK has been found to prefer NADH over NADPH as a cofactor *in vitro* (3, 7), our results demonstrate that SSA treatment significantly affected the intracellular ratio of NADPH/NADP but not of NADH/NAD, and the SSA-induced change in the NADPH/NADP ratio is heavily dependent on the functions encoded by *attKLM*.

SSA adapts bacteria to hydrogen peroxide protection. In various bacteria, nitrate assimilation and changes in the NADPH/NADP ratio are closely associated with the generation of reactive oxygen species (ROS) (35). ROS, such as a superoxide anion radical (O^{2-}), hydrogen peroxide (H_2O_2), and hydroxyl radicals (HO^-), are unavoidably generated during normal respiratory processes, and they can damage diverse cellular molecules (36). To protect against ROS-induced damage, bacteria have evolved sophisticated molecular mechanisms to sense ROS levels and synthesize enzymes such as catalase and superoxide dismutase (SOD), small proteins like thioredoxin (Trx) and glutaredoxin (Grx), and oligomeric proteins such as bacterioferritin (Bfr) (37–39). SOD catalyzes O^{2-} to H_2O_2 and H_2O, and catalase converts H_2O_2 to O_2 and H_2O_2, both of which directly reduce the toxicity of H_2O_2 and prevent the formation of hydroxyl radicals via the Fenton reaction (40). Trx and Grx are the protein disulfide reductases which serve as electron donors for enzymes such as peroxiredoxins (Prx) and sulfoxide reductases and therefore protect against oxidative damage (38, 41, 42). Bfr, on the other hand, oxidizes excess ferrous ions and protects bacterial cells against the oxidative stress associated with ferrous ions (43).

A. tumefaciens contains two catalases (KatA and CatE), three

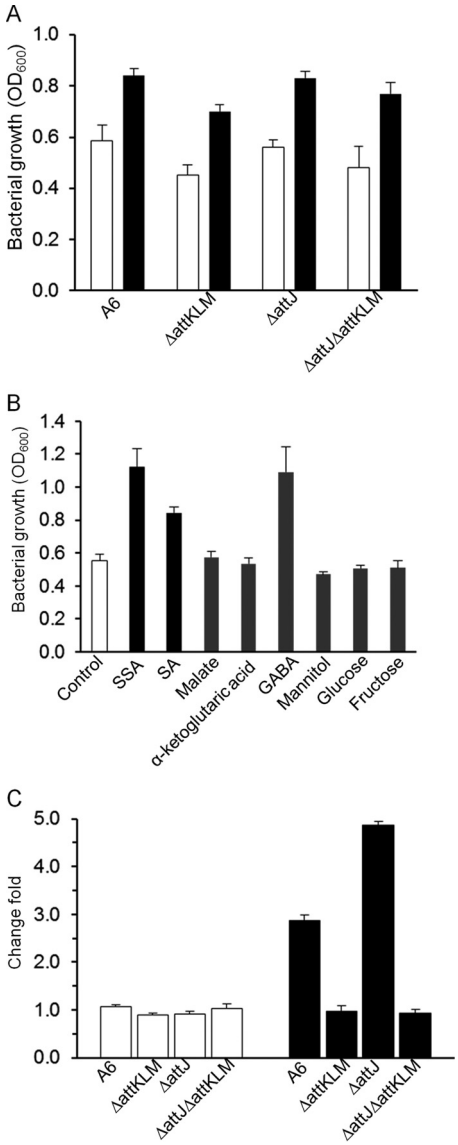

FIG 5 SA promotes nitrate utilization independent of *attJ-attKLM*. (A) Bacterial growth of A6 and its mutants using KNO_3 as the sole nitrogen source with (filled bars) or without (open bars) SA. (B) Bacterial growth of A6 using KNO_3 as the sole nitrogen source supplied by the given compounds. (C) Changes in the NADH/NAD (open bars) and NADPH/NADP (filled bars) ratios in *A. tumefaciens* A6 and its mutants upon SSA treatment.

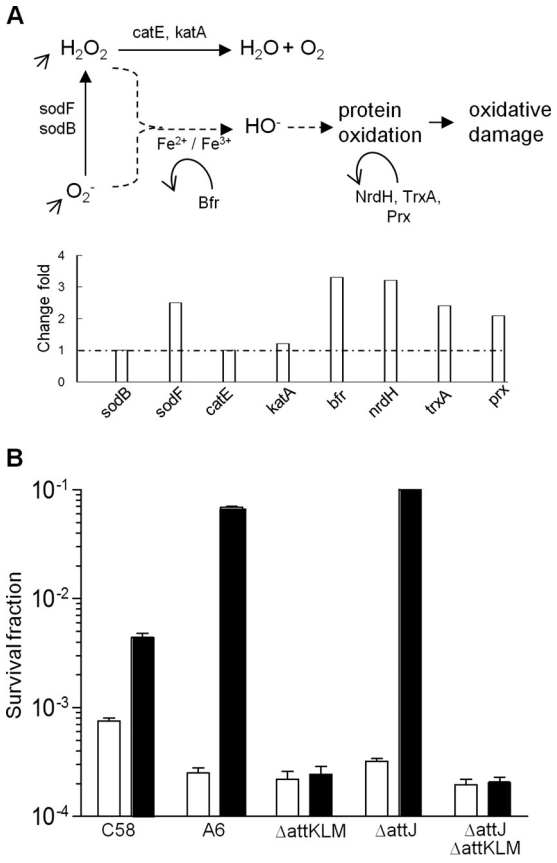

FIG 6 SSA induces oxidative stress resistance in *A. tumefaciens*. (A) Putative defense systems against oxidative stresses in *A. tumefaciens* and the expression profiles of related genes in microarray analysis. (B) SSA enhanced bacterial resistance against H_2O_2. The experiments were performed by adding 20 mM H_2O_2 to the fresh cell cultures with or without SSA induction. The cultures were then grown for an additional 30 min before aliquots of cells were removed, washed once prior to preparation of appropriate dilutions, and plated on LB agar. Colonies were counted after 48 h of incubation at 28°C. Surviving fractions were defined as the number of CFU recovered after the treatment divided by the number of CFU without treatment. Open bars, no SSA treatment; filled bars, SSA treatment. Error bars denote standard deviations.

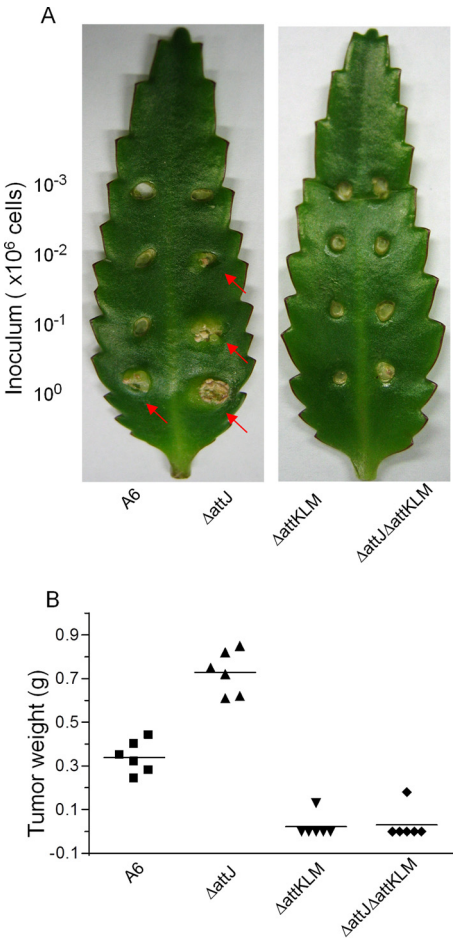

FIG 7 AttJ-AttKLM regulate the tumorigenicity of *A. tumefaciens*. (A) A representative photo for the tumorigenicity assay of *A. tumefaciens* A6 and its mutants. Bacteria were serially diluted 10-fold, and 5 μl of diluted samples was individually used to infect the leaves of *K. daigremontiana*. Arrows indicate visible tumor growth. (B) Tumor weights induced by *A. tumefaciens* A6 and its mutants.

SODs (SodB, SodF, and Atu4583), two Trxs (Atu0022 and Atu3698), two Grxs (Atu0068 and Atu3511), and three Prxs (Atu1480, Atu0779, and Atu2399) (44–46). Our microarray results showed that addition of SSA did not affect transcriptional expression of the genes encoding catalases and the regulator OxyR (47), indicating that direct detoxification of H_2O_2 is unlikely modulated by SSA in *A. tumefaciens*. However, the transcript levels of *sodF*, the Trx gene *atu0022*, the Grx gene *atu0068*, the Prx gene *atu0779*, and the Bfr gene *atu2771* were significantly elevated with SSA treatment (Fig. 6A), suggesting that SSA may be involved in regulation of oxidative protection. To test this possibility, we carried out an H_2O_2 killing assay and found that the SSA pretreatment could significantly protect bacterial cells against the oxidative reagent. As shown in Fig. 6B, preexposure of the nopaline strain C58 to SSA conferred a greater than 10-fold increase in resistance to the lethal dosage of H_2O_2 over levels in the untreated cells. Similar results were also observed for the octopine strain A6 (Fig. 6B). Mutation of *attJ* did not affect the SSA-induced bacterial resistance to H_2O_2. However, deletion of *attKLM* entirely abolished this SSA-mediated resistance (Fig. 6B), suggesting a key role of *attKLM* and SSA in modulation of the bacterial defense against oxidative stresses.

***attJ-attKLM* regulate the tumorigenicity of *A. tumefaciens*.** To further study the physiological role of *attJ-attKLM*, we analyzed bacterial virulence by infecting the plant host *Kalanchoe daigremontiana*. We grew the wild-type and mutant strains in LB medium. After cells were washed with PBS, different amounts of bacterial cells were inoculated into the wound sites of *K. daigremontiana*. We found that both the wild-type and Δ*attJ* mutant of octopine-type A6 readily incited plant tumors with an inoculum of 10^6 cells, while the Δ*attKLM* and Δ*attKLM*Δ*attJ* mutant strains hardly developed any plant tumors. With an inoculum of 10^5 cells, however, the wild type could not induce tumors, consistent with the previous results showing that the A6 strain is less virulent than the C58 strain. In contrast, the Δ*attJ* strain continued to induce tumors even with an inoculum of 10^4 cells, indicating a stronger virulence than that of the wild-type and the *attKLM* mutant strains (Fig. 7A). Analyses of tumor weights also confirmed that overexpression of *attKLM* by inactivation of the repressor gene

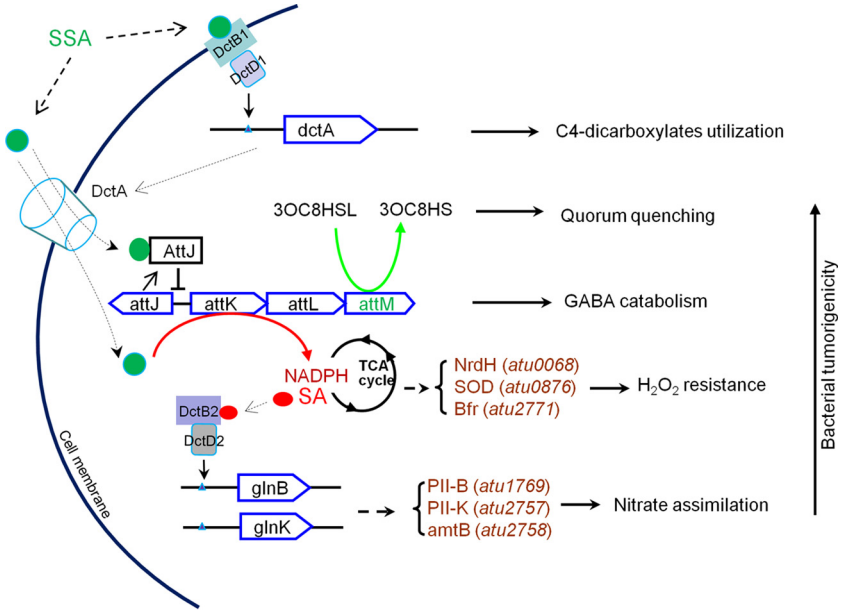

FIG 8 Schematic presentation of the genetic and physiological response to SSA in *A. tumefaciens*. Solid lines indicate the processes supported by experimental evidence, while dashed lines indicate speculative processes that await further experimental validation. 3OC8HS(L), 3-oxo-octanoyl-homoserine (lactone); PII, nitrogen regulatory protein.

attJ enhanced bacterial virulence and that mutation of *attKLM* impaired the development of plant tumors (Fig. 7B). These results appeared different from the findings of a previous study, in which the nopaline strain C58 was used to infect tobacco plants, and the results showed that the virulence of the *attM* mutant was similar to or even greater than that of the wild-type strain (4, 48). Strain specificity or a difference in host plants may explain this discrepancy, given that different plant hosts react differently to infections by different *A. tumefaciens* strains (49).

DISCUSSION

Previous results suggest that SSA, a metabolic intermediate of GABA, functions as a ligand of AttJ and induces the expression of *attKLM*, which leads to disruption of the QS signaling of *A. tumefaciens* during plant infections (4). However, a recent finding that *attKLM* does not affect Ti plasmid conjugation in plants argues the biological significance of SSA in regulation of bacterial virulence (50). In this study, we used the combined application of microarray and genetic analyses to understand the roles of SSA in regulation of bacterial physiology and virulence, and our results revealed three new biological functions influenced by SSA, i.e., promoting C_4-dicarboxylate utilization, nitrate assimilation, and ROS resistance in *A. tumefaciens*. Unlike its related metabolites GABA and SA, SSA could not support bacterial growth when supplied as the sole carbon source (Fig. 2), which seems to exclude the possibility that SSA promotes the utilization of malate and nitrate to support bacterial growth through its downstream metabolite SA.

In addition to modulation of quorum quenching and GABA metabolism, our results demonstrate that SSA plays additional roles through two different types of mechanisms to promote the bacterial survival capability (Fig. 8). First, SSA, independent of the *attJ-attKLM* genes, induces the expression of the C_4-dicarboxylate importer *dctA* and hence promotes the utilization of TCA intermediates (Fig. 2). It has been known that C_4-dicarboxylates are abundant in wound sites and plant tumors, and the transporter *dctA* is regulated by the two-component system DctB/DctD in bacteria (31). In its genome, *A. tumefaciens* carries two sets of the DctB/DctD pair, with one located on the cell membrane and one in the cytosol (see Fig. S3 in the supplemental material). Our results showed that SSA induced *dctA* transcription independent of the *attJ-attKLM* genes, suggesting that SSA may bind to the membrane-bound DctB/DctD and consequently induce the expression of DctA, which imports the plant-produced C_4-dicarboxylates, including SSA, leading to *attKLM* induction and utilization of C_4-dicarboxylates. Consistent with this notion, inactivation of *dctB1* reduced the bacterial growth rate when malate was supplied as the sole carbon source, and supplementation of SSA had no effect on the Δ*dctB1* strain (see Fig. S5 in the supplemental material). While these results demonstrate the importance of DctB1 in the SSA-mediated promotion of C_4-dicarboxylate utilization and nitrate assimilation, further characterization of DctB1 and DctB2 is required to provide a clear understanding of their physiological roles.

Second, our results revealed that SSA could promote nitrate assimilation in an *attJKLM*-dependent manner. Once inside bacterial cells, SSA acts as a signal directly binding to AttJ to activate the expression of *attKLM* (3), and their products AttK/AttL/AttM work together to metabolize GABA to support bacterial growth. Additionally, AttM functions as an AHL-lactonase to degrade QS signal and terminate or postpone the QS-dependent replication and conjugation of Ti plasmid (4, 8, 9, 48, 51). We showed in this study that conversion of SSA to SA could also influence the bacterial redox status, as reflected by the increased NADPH/NADP ratio, which was accompanied by enhanced nitrate assimilation (Fig. 3 to 6). Under normal conditions, nitrate is not a preferred nitrogen source for *A. tumefaciens*, but it is a major nitrogen source for plant growth and functions as a critical signal molecule

regulating the whole plant development process (52–54). Nitrate is mainly taken up from the soil by plant roots, stored in vacuoles, and accumulated at the wound sites for healing (55). It has been reported that nitrate is capable of increasing the number of tumors on inoculated plant hosts by 200% (56). During infection, *A. tumefaciens* inevitably encounters nutrient starvation, and it is conceivable that this bacterium has evolved the SSA-AttJKLM system to take advantage of the nitrate compounds. At present, the precise mechanism by which SSA promotes nitrate assimilation is not clear. In *A. tumefaciens*, genes for nitrate assimilation are mainly located in two clusters (see Fig. S2 in the supplemental material). Our microarray results show that the majority of these genes are upregulated by SSA. In various bacteria, nitrate-assimilating genes are regulated by the nitrogen-limiting sigma factor RpoN (57). Unlike other sigma factors such as RpoS and RpoH, RpoN requires an extra coactivator for gene activation (58). In the case of the nitrogen-assimilating genes, this coactivator has been identified as the response regulator of the DctB/DctD two-component system. Interestingly, sequence analyses revealed that *glnK* and *glnB*, like the *dctA* gene, contain typical DNA motifs for DctD binding in their promoter regions (see Fig. S4 in the supplemental material). Similar to *dctA*, SSA may activate the nitrate-assimilating genes by activating the DctB/DctD two-component system. However, unlike the expression of DctA, SSA-mediated nitrate assimilation is dependent on the function of *attKLM*, and the SSA-hydrolyzing product SA can also promote bacterial nitrate assimilation, suggesting that the intracellular SA but not SSA itself is the direct signal for this phenomenon. Given that two sets of the DctB/DctD system are present with different localizations in *A. tumefaciens*, it is most likely that one DctB/DctD pair specifically senses extracellular SSA on the cell membrane and that the other specifically senses intracellular SA in the bacterial cytosol. Intracellular SA may directly bind to DctB/DctD and activate the expression of *glnB* and *glnK*, thus inducing the nitrate response. It is also possible that SA, which was converted from SSA, revamps the central metabolism of *A. tumefaciens* and alters the level of other metabolic regulators such as glutamate and acetate, which are responsible for the nitrate response.

In addition to modulation of C_4-dicarboxylates and nitrate utilization, our results showed that SSA also contributes to ROS resistance and bacterial tumorigenicity (Fig. 6). For plants, a ROS burst is an early response to bacterial infection, where huge amounts of ROS are rapidly produced at the wound sites to directly kill the invading bacterial pathogens at the early stage of infection (59). Our results indicate that SSA could protect bacteria from killing by ROS. This finding results from the observation that conversion of SSA to SA is associated with the change in the NADPH/NADP ratio. NADPH usually serves as an electron donor for the respiratory chain; its oxidation inevitably produces ROS. At a sublethal concentration, ROS might trigger the protective mechanism of *A. tumefaciens* against subsequent oxidative stresses (60). It is not yet clear how SSA exactly activates this protective response. Given that the SSA-induced protection from ROS stress is dependent on the presence of *attKLM*, it is likely that SSA may need to be converted into succinate, which may increase the NADPH/NAD ratio and the ROS level and subsequently induce the expression of protective systems.

During a long history of coevolution with plants, *A. tumefaciens* has evolved complicated signaling and regulatory networks for establishing a successful infection. The SSA-regulated *attJ-attKLM* signaling pathway is one such example. The findings from this study allow us to propose a signaling and regulatory working model for SSA (Fig. 8). During A. *tumefaciens* infection, the plant-derived SSA is sensed by the membrane-bound sensor DctB1 of the bacterial pathogen, which leads to activation of the response regulator DctD1 and, consequently, induces the expression of *dctA*. The transporter DctA imports SSA into bacterial cells and induces the expression of *attKLM* by binding to the transcriptional repressor AttJ. While AttK/AttL/AttM work together to metabolize GBL to support bacterial growth as nitrogen and carbon sources, AttM also works alone as an AHL-lactonase to quench the QS system and provide fine control of the bacterial energy-consuming processes, such as Ti plasmid replication and conjugation. In addition, expressed AttK converts SSA into SA, which not only detoxifies the high concentration of SSA but also influences the NADPH/NADP ratio. Functioning as an intracellular signal, SA is sensed by the cytosolic sensor DctB2 and activates the corresponding regulator DctD2, which subsequently expresses the nitrate-assimilating genes and promotes bacterial resistance to oxidative stresses. While the detailed molecular mechanisms of this working model await further experimental validation, it is clear from the findings of this study that SSA could be a potent plant signal which modulates bacterial physiology and contributes to the survival capability and tumorigenicity of *A. tumefaciens* during infection.

ACKNOWLEDGMENTS

This work was partially supported by the Singapore Biomedical Research Council (A*STAR), the National Basic Research Program of China (973 Program, number 2015CB150600), and the Singapore National Research Foundation (NRF-RF2009-RF001-267).

We declare that we have no conflicts of interest.

REFERENCES

1. **Subramoni S, Nathoo N, Klimov E, Yuan ZC.** 2014. *Agrobacterium tumefaciens* responses to plant-derived signaling molecules. Front Plant Sci **5:**322. http://dx.doi.org/10.3389/fpls.2014.00322.
2. **Zhang HB, Wang C, Zhang LH.** 2004. The quormone degradation system of *Agrobacterium tumefaciens* is regulated by starvation signal and stress alarmone (p)ppGpp. Mol Microbiol **52:**1389–1401. http://dx.doi.org/10.1111/j.1365-2958.2004.04061.x.
3. **Wang C, Zhang HB, Wang LH, Zhang LH.** 2006. Succinic semialdehyde couples stress response to quorum-sensing signal decay in *Agrobacterium tumefaciens*. Mol Microbiol **62:**45–56. http://dx.doi.org/10.1111/j.1365-2958.2006.05351.x.
4. **Chevrot R, Rosen R, Haudecoeur E, Cirou A, Shelp BJ, Ron E, Faure D.** 2006. GABA controls the level of quorum-sensing signal in *Agrobacterium tumefaciens*. Proc Natl Acad Sci U S A **103:**7460–7464. http://dx.doi.org/10.1073/pnas.0600313103.
5. **Yuan ZC, Haudecoeur E, Faure D, Kerr KF, Nester EW.** 2008. Comparative transcriptome analysis of *Agrobacterium tumefaciens* in response to plant signal salicylic acid, indole-3-acetic acid and gamma-amino butyric acid reveals signalling cross-talk and *Agrobacterium*-plant coevolution. Cell Microbiol **10:**2339–2354. http://dx.doi.org/10.1111/j.1462-5822.2008.01215.x.
6. **Carlier A, Chevrot R, Dessaux Y, Faure D.** 2004. The assimilation of gamma-butyrolactone in *Agrobacterium tumefaciens* C58 interferes with the accumulation of the *N*-acyl-homoserine lactone signal. Mol Plant Microbe Interact **17:**951–957. http://dx.doi.org/10.1094/MPMI.2004.17.9.951.
7. **Chai Y, Tsai CS, Cho H, Winans SC.** 2007. Reconstitution of the biochemical activities of the AttJ repressor and the AttK, AttL, and AttM catabolic enzymes of *Agrobacterium tumefaciens*. J Bacteriol **189:**3674–3679. http://dx.doi.org/10.1128/JB.01274-06.
8. **Zhang HB, Wang LH, Zhang LH.** 2002. Genetic control of quorum-

sensing signal turnover in *Agrobacterium tumefaciens*. Proc Natl Acad Sci U S A **99:**4638–4643. http://dx.doi.org/10.1073/pnas.022056699.
9. **Pappas KM.** 2008. Cell-cell signaling and the *Agrobacterium tumefaciens* Ti plasmid copy number fluctuations. Plasmid **60:**89–107. http://dx.doi.org/10.1016/j.plasmid.2008.05.003.
10. **Pan Y, Fiscus V, Meng W, Zheng Z, Zhang LH, Fuqua C, Chen L.** 2011. The *Agrobacterium tumefaciens* transcription factor BlcR is regulated via oligomerization. J Biol Chem **286:**20431–20440. http://dx.doi.org/10.1074/jbc.M110.196154.
11. **Molina-Henares AJ, Krell T, Eugenia Guazzaroni M, Segura A, Ramos JL.** 2006. Members of the IclR family of bacterial transcriptional regulators function as activators and/or repressors. FEMS Microbiol Rev **30:**157–186. http://dx.doi.org/10.1111/j.1574-6976.2005.00008.x.
12. **Liu Y, Jiang G, Cui Y, Mukherjee A, Ma WL, Chatterjee AK.** 1999. $kdgR_{Ecc}$ negatively regulates genes for pectinases, cellulase, protease, $Harpin_{Ecc}$, and a global RNA regulator in *Erwinia carotovora* subsp. *carotovora*. J Bacteriol **181:**2411–2421.
13. **Maloy SR, Nunn WD.** 1982. Genetic regulation of the glyoxylate shunt in *Escherichia coli* K-12. J Bacteriol **149:**173–180.
14. **Nasser W, Reverchon S, Robert-Baudouy J.** 1992. Purification and functional characterization of the KdgR protein, a major repressor of pectinolysis genes of *Erwinia chrysanthemi*. Mol Microbiol **6:**257–265. http://dx.doi.org/10.1111/j.1365-2958.1992.tb02007.x.
15. **Sunnarborg A, Klumpp D, Chung T, LaPorte DC.** 1990. Regulation of the glyoxylate bypass operon: cloning and characterization of *iclR*. J Bacteriol **172:**2642–2649.
16. **van Wezel GP, van der Meulen J, Kawamoto S, Luiten RG, Koerten HK, Kraal B.** 2000. *ssgA* is essential for sporulation of *Streptomyces coelicolor* A3(2) and affects hyphal development by stimulating septum formation. J Bacteriol **182:**5653–5662. http://dx.doi.org/10.1128/JB.182.20.5653-5662.2000.
17. **Gupta M, Hogema BM, Grompe M, Bottiglieri TG, Concas A, Biggio G, Sogliano C, Rigamonti AE, Pearl PL, Snead OC, III, Jakobs C, Gibson KM.** 2003. Murine succinate semialdehyde dehydrogenase deficiency. Ann Neurol **54**(Suppl 6):S81–S90. http://dx.doi.org/10.1002/ana.10625.
18. **Yogeeswari P, Sriram D, Vaigundaragavendran J.** 2005. The GABA shunt: an attractive and potential therapeutic target in the treatment of epileptic disorders. Curr Drug Metab **6:**127–139. http://dx.doi.org/10.2174/1389200053586073.
19. **Bouche N, Fait A, Bouchez D, Moller SG, Fromm H.** 2003. Mitochondrial succinic-semialdehyde dehydrogenase of the gamma-aminobutyrate shunt is required to restrict levels of reactive oxygen intermediates in plants. Proc Natl Acad Sci U S A **100:**6843–6848. http://dx.doi.org/10.1073/pnas.1037532100.
20. **Fait A, Yellin A, Fromm H.** 2005. GABA shunt deficiencies and accumulation of reactive oxygen intermediates: insight from *Arabidopsis* mutants. FEBS Lett **579:**415–420. http://dx.doi.org/10.1016/j.febslet.2004.12.004.
21. **Coleman ST, Fang TK, Rovinsky SA, Turano FJ, Moye-Rowley WS.** 2001. Expression of a glutamate decarboxylase homologue is required for normal oxidative stress tolerance in *Saccharomyces cerevisiae*. J Biol Chem **276:**244–250. http://dx.doi.org/10.1074/jbc.M007103200.
22. **Lutke-Eversloh T, Steinbuchel A.** 1999. Biochemical and molecular characterization of a succinate semialdehyde dehydrogenase involved in the catabolism of 4-hydroxybutyric acid in *Ralstonia eutropha*. FEMS Microbiol Lett **181:**63–71. http://dx.doi.org/10.1111/j.1574-6968.1999.tb08827.x.
23. **Wilms I, Voss B, Hess WR, Leichert LI, Narberhaus F.** 2011. Small RNA-mediated control of the *Agrobacterium tumefaciens* GABA binding protein. Mol Microbiol **80:**492–506. http://dx.doi.org/10.1111/j.1365-2958.2011.07589.x.
24. **Goodner B, Hinkle G, Gattung S, Miller N, Blanchard M, Qurollo B, Goldman BS, Cao Y, Askenazi M, Halling C, Mullin L, Houmiel K, Gordon J, Vaudin M, Iartchouk O, Epp A, Liu F, Wollam C, Allinger M, Doughty D, Scott C, Lappas C, Markelz B, Flanagan C, Crowell C, Gurson J, Lomo C, Sear C, Strub G, Cielo C, Slater S.** 2001. Genome sequence of the plant pathogen and biotechnology agent *Agrobacterium tumefaciens* C58. Science **294:**2323–2328. http://dx.doi.org/10.1126/science.1066803.
25. **Wood DW, Setubal JC, Kaul R, Monks DE, Kitajima JP, Okura VK, Zhou Y, Chen L, Wood GE, Almeida NF, Jr, Woo L, Chen Y, Paulsen IT, Eisen JA, Karp PD, Bovee D, Sr, Chapman P, Clendenning J, Deatherage G, Gillet W, Grant C, Kutyavin T, Levy R, Li MJ, McClelland E, Palmieri A, Raymond C, Rouse G, Saenphimmachak C, Wu Z, Romero P, Gordon D, Zhang S, Yoo H, Tao Y, Biddle P, Jung M, Krespan W, Perry M, Gordon-Kamm B, Liao L, Kim S, Hendrick C, Zhao ZY, Dolan M, Chumley F, Tingey SV, Tomb JF, Gordon MP, Olson MV, Nester EW.** 2001. The genome of the natural genetic engineer *Agrobacterium tumefaciens* C58. Science **294:**2317–2323. http://dx.doi.org/10.1126/science.1066804.
26. **Irizarry RA, Hobbs B, Collin F, Beazer-Barclay YD, Antonellis KJ, Scherf U, Speed TP.** 2003. Exploration, normalization, and summaries of high density oligonucleotide array probe level data. Biostatistics **4:**249–264. http://dx.doi.org/10.1093/biostatistics/4.2.249.
27. **Metcalf WW, Jiang W, Daniels LL, Kim SK, Haldimann A, Wanner BL.** 1996. Conditionally replicative and conjugative plasmids carrying *lacZ*α for cloning, mutagenesis, and allele replacement in bacteria. Plasmid **35:**1–13. http://dx.doi.org/10.1006/plas.1996.0001.
28. **Garfinkel DJ, Nester EW.** 1980. *Agrobacterium tumefaciens* mutants affected in crown gall tumorigenesis and octopine catabolism. J Bacteriol **144:**732–743.
29. **Spaink HP.** 1995. The molecular basis of infection and nodulation by rhizobia: the ins and outs of sympathogenesis. Annu Rev Phytopathol **33:**345–368. http://dx.doi.org/10.1146/annurev.py.33.090195.002021.
30. **Wu ZL, Charles TC, Wang H, Nester EW.** 1992. The *ntrA* gene of *Agrobacterium tumefaciens*: identification, cloning, and phenotype of a site-directed mutant. J Bacteriol **174:**2720–2723.
31. **Yurgel SN, Kahn ML.** 2004. Dicarboxylate transport by rhizobia. FEMS Microbiol Rev **28:**489–501. http://dx.doi.org/10.1016/j.femsre.2004.04.002.
32. **Ronson CW, Nixon BT, Albright LM, Ausubel FM.** 1987. *Rhizobium meliloti ntrA* (*rpoN*) gene is required for diverse metabolic functions. J Bacteriol **169:**2424–2431.
33. **Lin JT, Stewart V.** 1998. Nitrate assimilation by bacteria. Adv Microb Physiol **39:**1–30, 379.
34. **Spaink HP, Kondorosi A, Hooykaas PJJ.** 1998. The *Rhizobiaceae*: molecular biology of model plant-associated bacteria. Kluwer Academic Publishers, Boston, MA.
35. **Shimizu K.** 2013. Metabolic regulation of a bacterial cell system with emphasis on *Escherichia coli* metabolism. ISRN Biochem **2013:**645983. http://dx.doi.org/10.1155/2013/645983.
36. **Imlay JA.** 2013. The molecular mechanisms and physiological consequences of oxidative stress: lessons from a model bacterium. Nat Rev Microbiol **11:**443–454. http://dx.doi.org/10.1038/nrmicro3032.
37. **Harrison J, Jamet A, Muglia CI, Van de Sype G, Aguilar OM, Puppo A, Frendo P.** 2005. Glutathione plays a fundamental role in growth and symbiotic capacity of *Sinorhizobium meliloti*. J Bacteriol **187:**168–174. http://dx.doi.org/10.1128/JB.187.1.168-174.2005.
38. **Hofmann B, Hecht HJ, Flohe L.** 2002. Peroxiredoxins. Biol Chem **383:**347–364.
39. **Steinman HM, Fareed F, Weinstein L.** 1997. Catalase-peroxidase of *Caulobacter crescentus*: function and role in stationary-phase survival. J Bacteriol **179:**6831–6836.
40. **McCord JM, Fridovich I.** 1969. The utility of superoxide dismutase in studying free radical reactions. I. Radicals generated by the interaction of sulfite, dimethyl sulfoxide, and oxygen. J Biol Chem **244:**6056–6063.
41. **Arner ES, Holmgren A.** 2000. Physiological functions of thioredoxin and thioredoxin reductase. Eur J Biochem **267:**6102–6109. http://dx.doi.org/10.1046/j.1432-1327.2000.01701.x.
42. **Rodriguez-Manzaneque MT, Ros J, Cabiscol E, Sorribas A, Herrero E.** 1999. Grx5 glutaredoxin plays a central role in protection against protein oxidative damage in *Saccharomyces cerevisiae*. Mol Cell Biol **19:**8180–8190. http://dx.doi.org/10.1128/MCB.19.12.8180.
43. **Smith JL.** 2004. The physiological role of ferritin-like compounds in bacteria. Crit Rev Microbiol **30:**173–185. http://dx.doi.org/10.1080/10408410490435151.
44. **Prapagdee B, Eiamphungporn W, Saenkham P, Mongkolsuk S, Vattanaviboon P.** 2004. Analysis of growth phase regulated KatA and CatE and their physiological roles in determining hydrogen peroxide resistance in *Agrobacterium tumefaciens*. FEMS Microbiol Lett **237:**219–226. http://dx.doi.org/10.1111/j.1574-6968.2004.tb09699.x.
45. **Xu XQ, Pan SQ.** 2000. An *Agrobacterium* catalase is a virulence factor involved in tumorigenesis. Mol Microbiol **35:**407–414. http://dx.doi.org/10.1046/j.1365-2958.2000.01709.x.
46. **Eiamphungporn W, Nakjarung K, Prapagdee B, Vattanaviboon P, Mongkolsuk S.** 2003. Oxidant-inducible resistance to hydrogen peroxide killing in *Agrobacterium tumefaciens* requires the global peroxide sensor-

regulator OxyR and KatA. FEMS Microbiol Lett **225:**167–172. http://dx.doi.org/10.1016/S0378-1097(03)00511-1.
47. **Nakjarung K, Mongkolsuk S, Vattanaviboon P.** 2003. The *oxyR* from *Agrobacterium tumefaciens*: evaluation of its role in the regulation of catalase and peroxide responses. Biochem Biophys Res Commun **304:**41–47. http://dx.doi.org/10.1016/S0006-291X(03)00535-7.
48. **Haudecoeur E, Planamente S, Cirou A, Tannieres M, Shelp BJ, Morera S, Faure D.** 2009. Proline antagonizes GABA-induced quenching of quorum-sensing in *Agrobacterium tumefaciens*. Proc Natl Acad Sci U S A **106:**14587–14592. http://dx.doi.org/10.1073/pnas.0808005106.
49. **Ooms G, Klapwijk PM, Poulis JA, Schilperoort RA.** 1980. Characterization of Tn904 insertions in octopine Ti plasmid mutants of *Agrobacterium tumefaciens*. J Bacteriol **144:**82–91.
50. **Khan SR, Farrand SK.** 2009. The BlcC (AttM) lactonase of *Agrobacterium tumefaciens* does not quench the quorum-sensing system that regulates Ti plasmid conjugative transfer. J Bacteriol **191:**1320–1329. http://dx.doi.org/10.1128/JB.01304-08.
51. **Haudecoeur E, Faure D.** 2010. A fine control of quorum-sensing communication in *Agrobacterium tumefaciens*. Commun Integr Biol **3:**84–88. http://dx.doi.org/10.4161/cib.3.2.10429.
52. **Wang YY, Tsay YF.** 2011. *Arabidopsis* nitrate transporter NRT1.9 is important in phloem nitrate transport. Plant Cell **23:**1945–1957. http://dx.doi.org/10.1105/tpc.111.083618.
53. **Gojon A, Krouk G, Perrine-Walker F, Laugier E.** 2011. Nitrate transceptor(s) in plants. J Exp Bot **62:**2299–2308. http://dx.doi.org/10.1093/jxb/erq419.
54. **Vidal EA, Gutierrez RA.** 2008. A systems view of nitrogen nutrient and metabolite responses in *Arabidopsis*. Curr Opin Plant Biol **11:**521–529. http://dx.doi.org/10.1016/j.pbi.2008.07.003.
55. **Song J, Ding X, Feng G, Zhang F.** 2006. Nutritional and osmotic roles of nitrate in a euhalophyte and a xerophyte in saline conditions. New Phytol **171:**357–366. http://dx.doi.org/10.1111/j.1469-8137.2006.01748.x.
56. **Khalfa MDE, Lippincott JA.** 1968. Promotion of crown-gall tumor initiation on primary pinto bean leaves by certain inorganic salts. Plant Cell Physiol **9:**217–225.
57. **Fischer HM.** 1994. Genetic regulation of nitrogen fixation in rhizobia. Microbiol Rev **58:**352–386.
58. **Dombrecht B, Marchal K, Vanderleyden J, Michiels J.** 2002. Prediction and overview of the RpoN-regulon in closely related species of the *Rhizobiales*. Genome Biol **3:**RESEARCH0076. http://dx.doi.org/10.1186/gb-2002-3-12-research0076.
59. **Wojtaszek P.** 1997. Oxidative burst: an early plant response to pathogen infection. Biochem J **322:**681–692. http://dx.doi.org/10.1042/bj3220681.
60. **Xu XQ, Li LP, Pan SQ.** 2001. Feedback regulation of an *Agrobacterium* catalase gene *katA* involved in *Agrobacterium*-plant interaction. Mol Microbiol **42:**645–657.